Ravi Subrahmanyan
CSIRO-CASS, Curtin-CIRA
March 2021

AAVS2 antenna total powers versus time at 110 MHz

AAVS2 is an array of 256 SKALA4.1 antennas distributed in a semi-random manner over a circular station area, with maximum spacing of 38 metres. The SKALA4.1 antenna is of dual linear polarisation and all antennas in the station are oriented with X polarisation along EW and Y polarisation along NS.

In this note the analysis is of total power data acquired with X and Y polarisation feeds of the SKALA4.1 antennas, recorded over 24 hours beginning 10:20 UT or 18:20 local time, on 21/04/2020. Analysis is done of data at 110 MHz, which lies close to the geometric centre of the SKA Low band.

During the 24 hr observation, a pair of total power samples were recorded every 5 mins. Each data sample in the pair has integration time 0.14 sec, and the pair of data are at adjacent times. The data are in 32 fine channels of 28.935 kHz, giving a 0.926-MHz bandwidth centred at 110.13 MHz. For this analysis, the amplitudes of all channel data were averaged together to form a single total power estimate, without any bandpass calibration. Data with obvious RFI or clearly unstable receiver chains were rejected.

The antenna locations are shown, for reference, in the figure below, with antenna numbering corresponding to that used in the EM modelling (file: AAVS2_loc_italia_190429.txt). This antenna numbering scheme is used throughout this note.

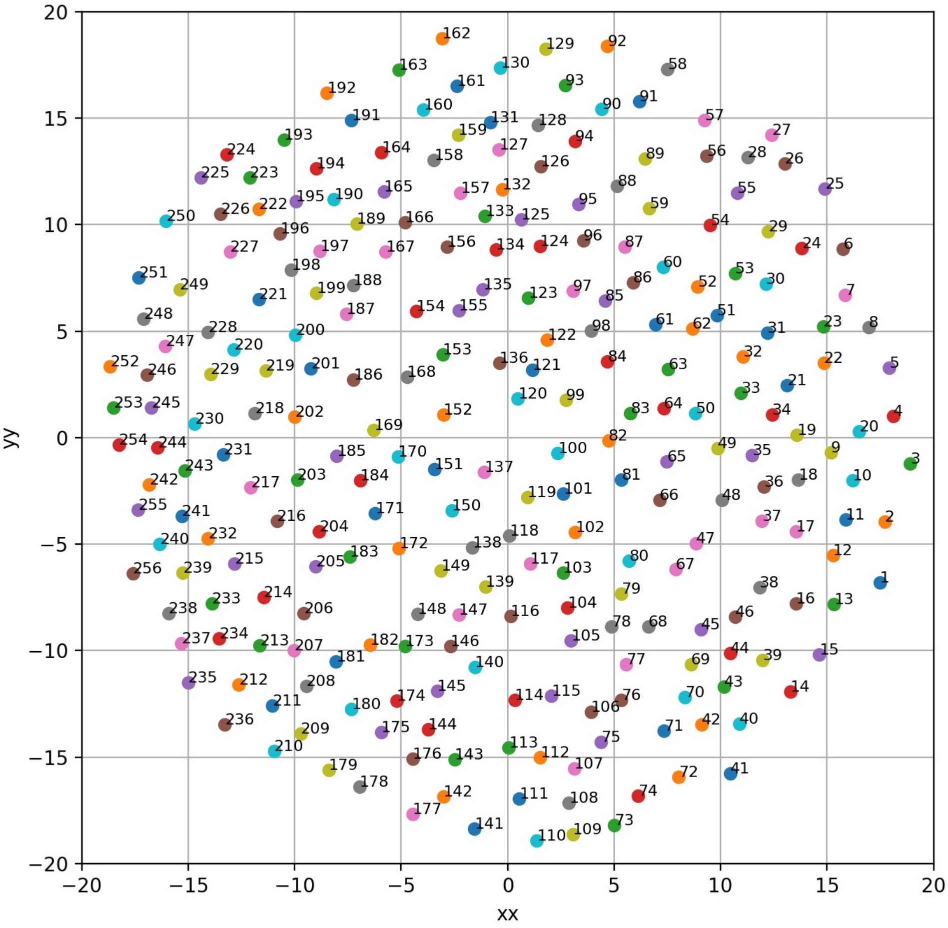

I used the GDSM all-sky model (Zheng et al. 2016) implemented in PyGSM, to get an all-sky brightness distribution model at the band centre frequency. The healpix image was degraded to "side" of 16 corresponding to 219.87 arcmin pixels. This resolution was sufficient given the angular scale of structure in the embedded element patterns; additionally, it was confirmed that the results presented below are not limited by the coarse resolution of the sky model. The coarse resolution also allowed computations to be completed in my MacBook Pro in reasonable time.

The Sun was included in the all-sky model using the flux density in Benz (2009), which represents the thermal emission in quiet state. The sky position of the Sun was computed from astronomical ephemeris at each time and the healpix pixel where it was located was added an equivalent brightness temperature.

Embedded element patterns (EEP) for all 256 antennas in the station are from the FEKO analysis done for the SKALA4.1 antenna in AAVS2 configuration and at 110 MHz. The total power patterns for X and Y polarisations are used. Patterns are shown below for 16 antennas, to serve as examples and for reference. The colour scale is linear in power and each 2D beam pattern has been normalised to have peak of unity.

X-polarisation beam patterns:

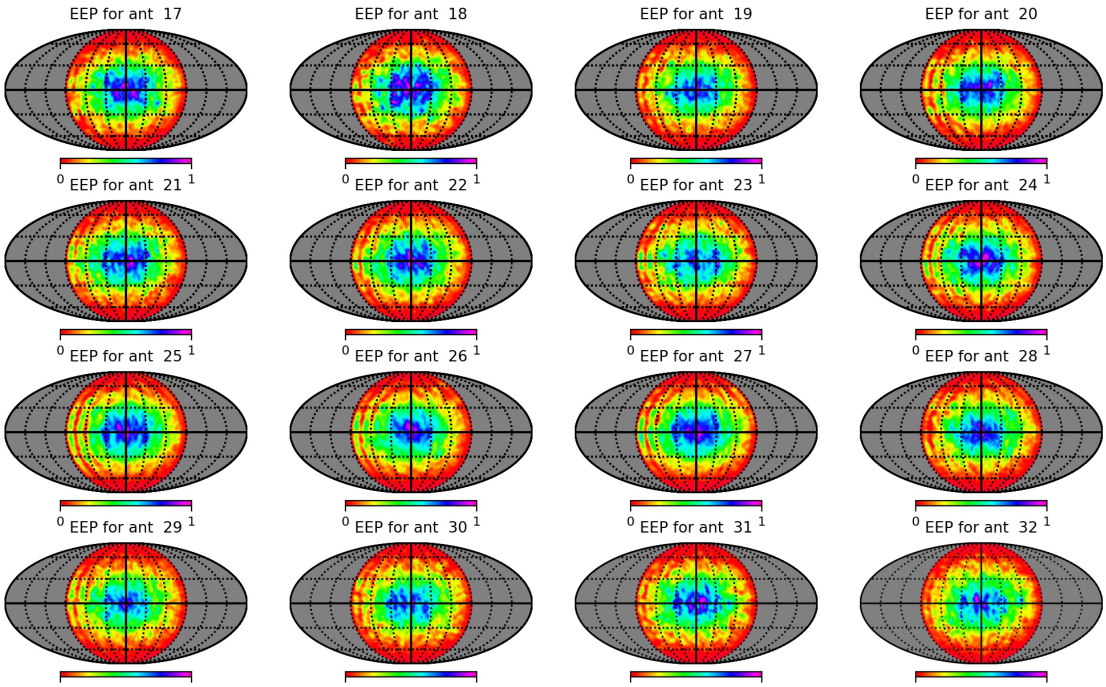

Y-polarisation beam patterns:

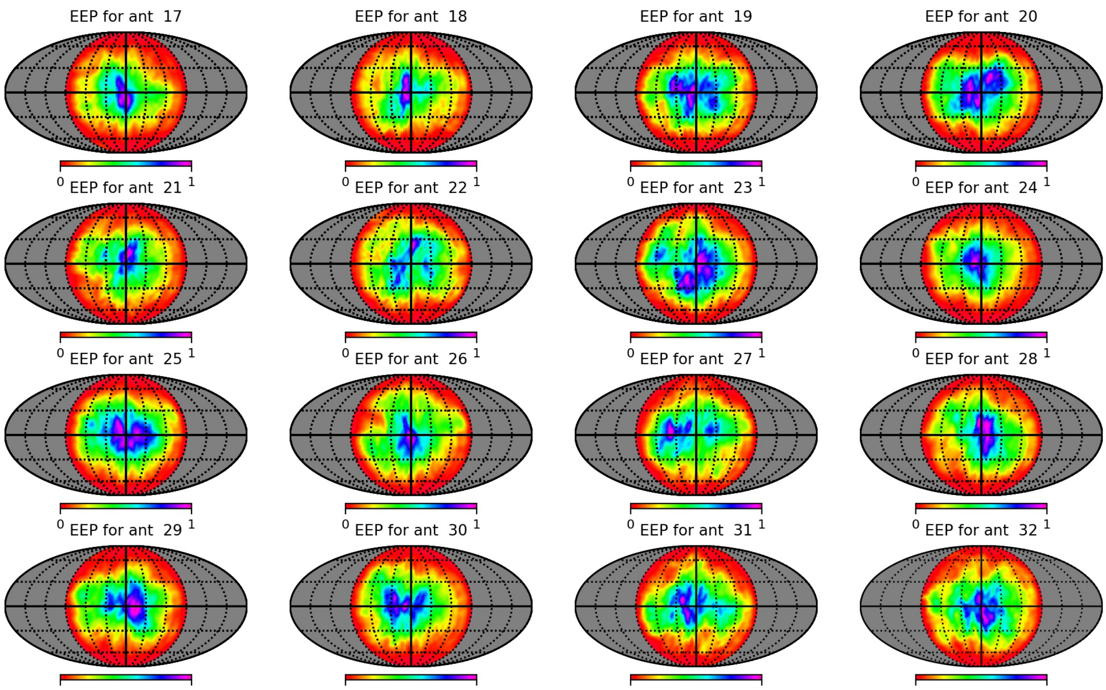

I convolved the model sky with the EEP beam patterns to derive traces of total power versus time, for the site location on Earth, and compared with the data. There is expected to be a scaling required to convert the measured data counts to kelvin brightness temperature. Additionally, the data would have an offset, representing the receiver noise and thermal emission from any resistive losses in the antenna and transmission line connecting to the first low-noise amplifier. Allowing for offset and scaling, I found that a good match between model and measurement required allowing for a common-mode drift in receiver gain versus time. This drift was solved for using the data and model, separately for X and Y polarisations.

Given below is the computed common-mode drift in gain of the receiver chains in X polarisation:

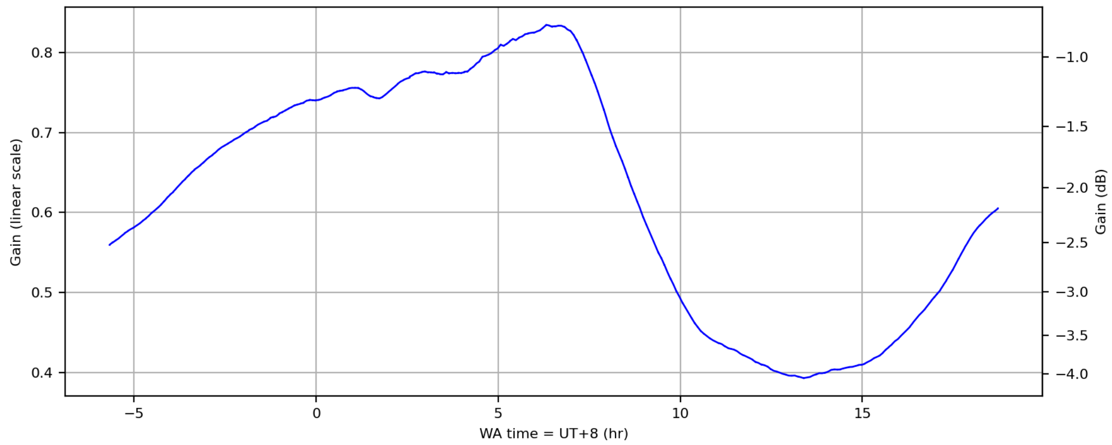

And below is the corresponding plot for Y polarisation:

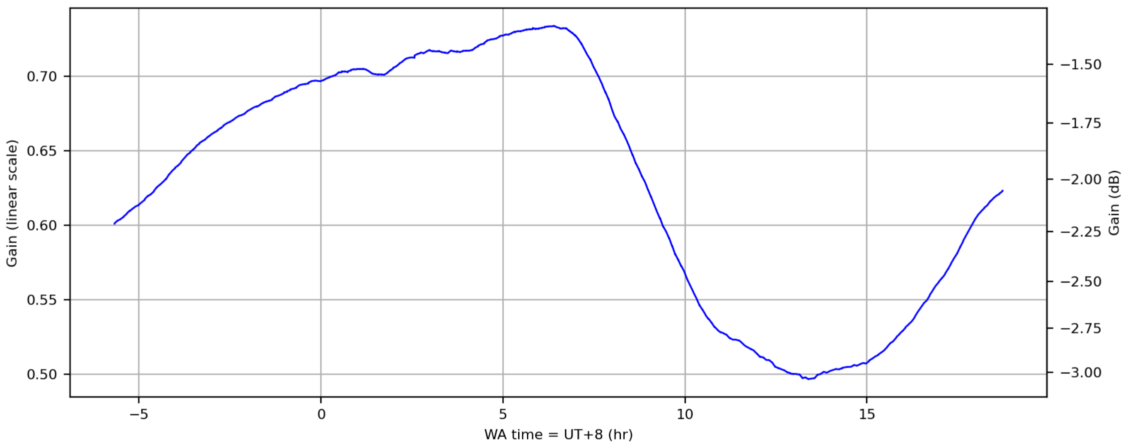

The two plots are similar, except for the y-axis scale. The data acquisition begins at a time close to sunset and the total duration is close to 24 hrs. The first half of the observing time, which is night-time, sees the system gain increasing, presumably as the ambient temperature cools during the night. In the hours following sunrise till just after midday the gain drops, presumably as the ambient temperature rises. Late afternoon and evening as the ambient temperature cools the gain rises, now at a rate more than that at night. Close to sunset the rate of increase in gain reduces once again to that at night time.

Quantitatively, the peak-to-peak change in gain is close to 3 dB for the X polarisation channels and close to 1.75 dB for the Y polarisation channels.

Looking at SKA-TEL-SKO-0001088 REPORT ON THE STATION CALIBRATION TASK, I see that laboratory tests have shown that the gains in the LNA module and also FEM do drop with increasing temperature. The laboratory measurements showed a sensitivity of 0.05 dB/degree C in X polarisation and about 0.1 dB/degree C in Y polarisation. The 1.75-3 dB peak-to-peak change in gain over the day and night is to be expected given that the FEM box temperature might vary over a few 10's of degrees C over any 24 hour period. However, the data analysed in this report shows greater sensitivity of gain to temperature for X polarisation (1270 nm carrier), whereas laboratory measurements show greater sensitivity in the Y polarisation channel (with a 1330 nm carrier).

The data were corrected for the above common-mode gain changes. Subsequently, temperature versus temperature T-T plots were made, plotting predictions from global sky model versus data, for each antenna and polarisation separately. These are shown below for X and Y polarisations:

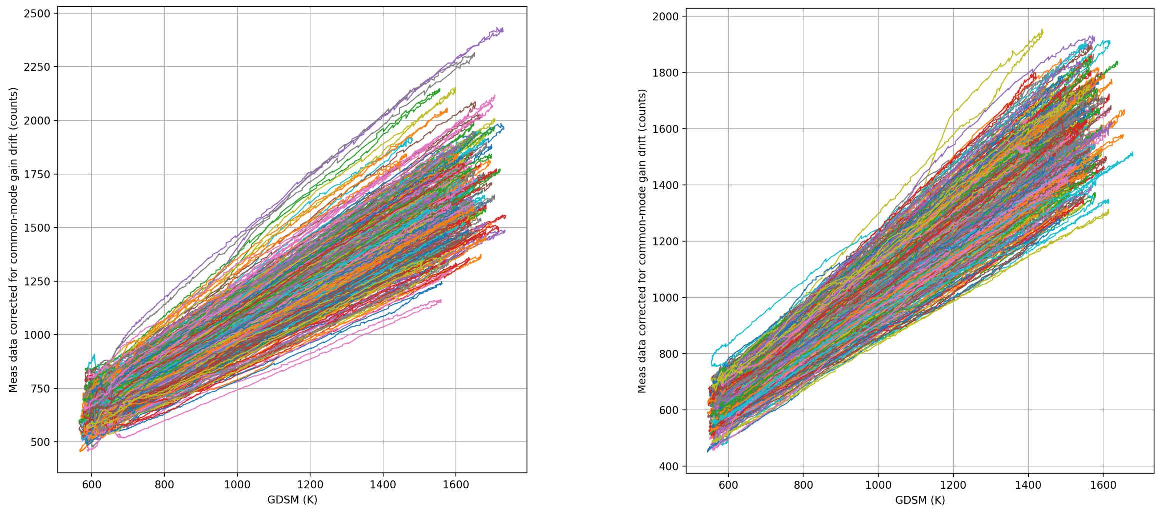

Most individual antennas are well represented by straight lines that have different slopes, because different antennas would have different scaling factors that transform their counts to kelvin units. Straight line fits are made to these T-T scatter plots, to yield an offset and scaling factor for each antenna and polarisation.

The offsets have mean values 40 K in X polarisation and 42 K in Y polarisation, consistent with the expected receiver temperature of 40 K in both X and Y polarisations (It may be noted here that this is not an independent measurement of receiver noise temperature because the derivation of common mode gain presented above makes the assumption that the receiver noise is 40 K).

The total power counts in each antenna and polarisation are separately given an offset and scale using the above factors, derived from the fits, to convert to antenna temperatures in kelvin units. Following this calibration, the temperature versus temperature T-T plots of sky model predictions versus calibrated data are as follows, in the X and Y polarisations:

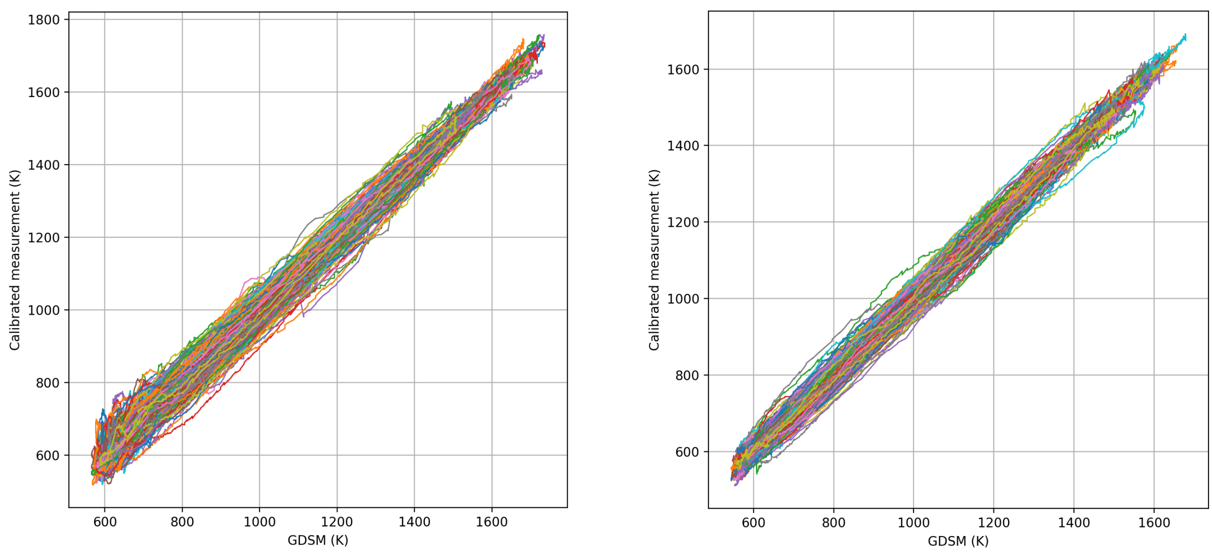

The fits are reasonably good, the match between predictions and data is somewhat better in y polarisation.

Shown below are plots of the calibrated antenna temperature measurements versus time for all the antennas in the station, along with the differences between antenna temperature measurements and model predictions.

For X polarisation:

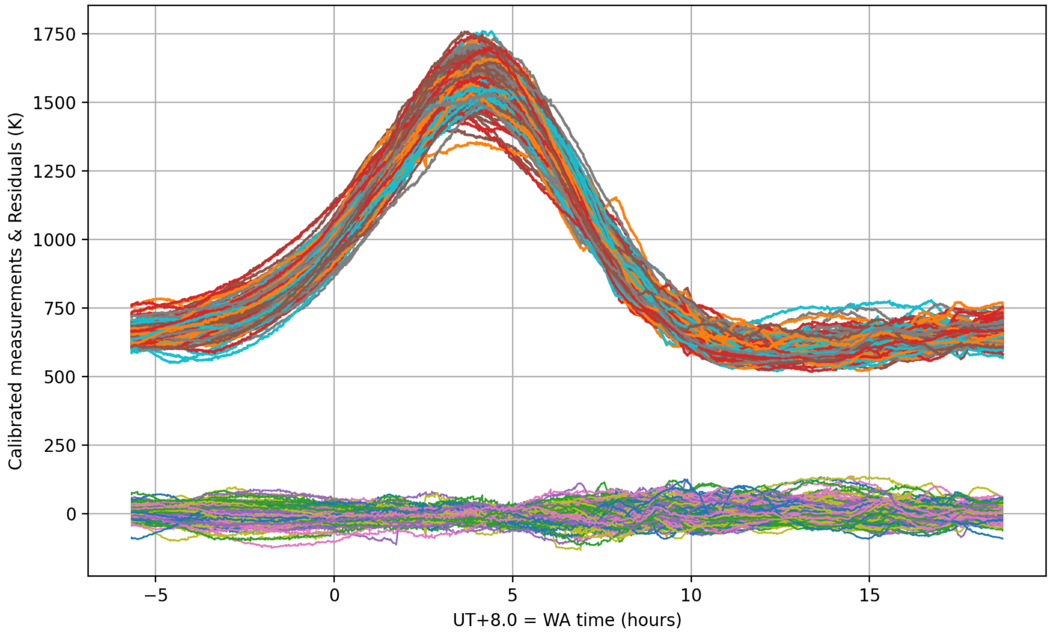

And for Y polarisation:

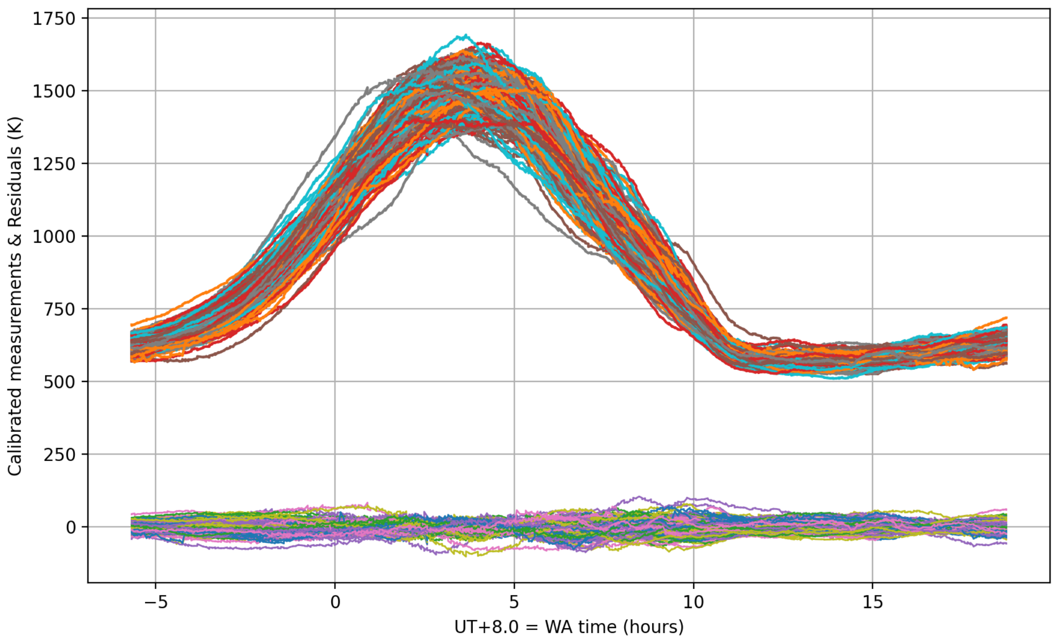

Notice that the thickness of the bundle of traces representing the residuals—difference between calibrated measurements and model predictions—is significantly smaller than the thickness of the bundle of traces representing the calibrated measurements. The embedded patterns do vary across the antennas in the station, and hence the calibrated measurements as well as the predictions of antenna temperature versus time do vary from antenna to antenna within the station.

An indication of the goodness of the computed embedded patterns, as well as goodness of the global sky model, is the match between calibrated measurements of antenna temperature versus time with predictions made using EEP beam patterns along with the global sky model, including the Sun.

There is no systematic error in the residuals, either in X or Y polarisation. The fractional error is greatest during daytime when uncorrelated gain variations in the receiver chain currently limit calibration accuracy. Nevertheless, the RMS difference between the calibrated data and predictions from global sky model is less than 5% in X and 3% in Y polarisation. Shown below are overlays of measurement (blue) and predictions (red) for 16 antennas in the station:

In X polarisation:

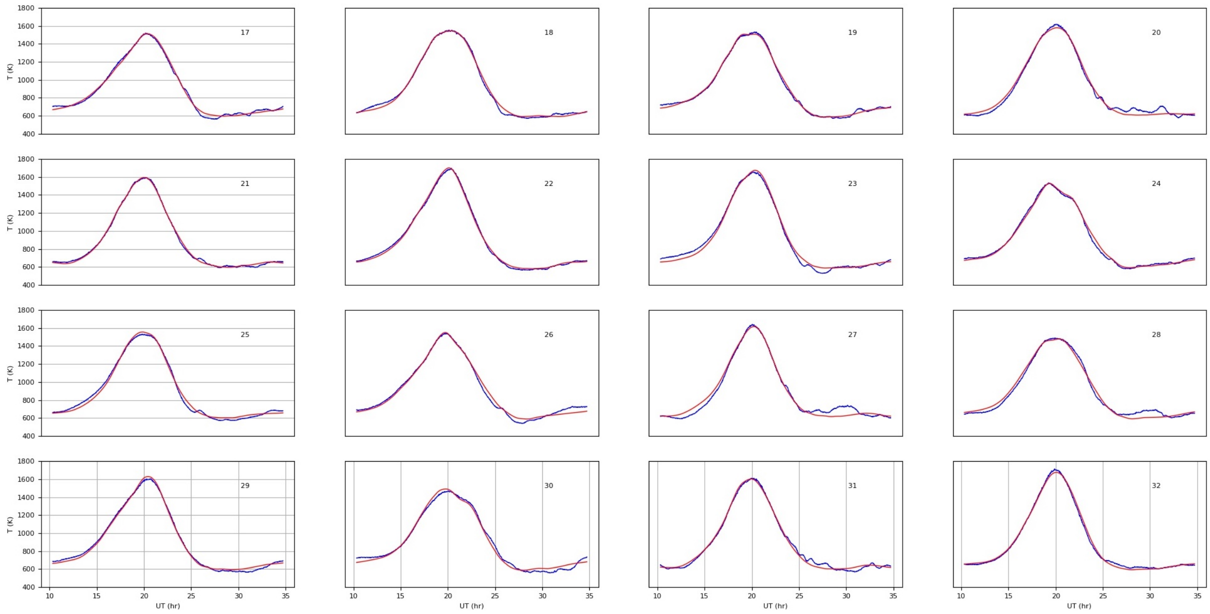

In Y polarisation:

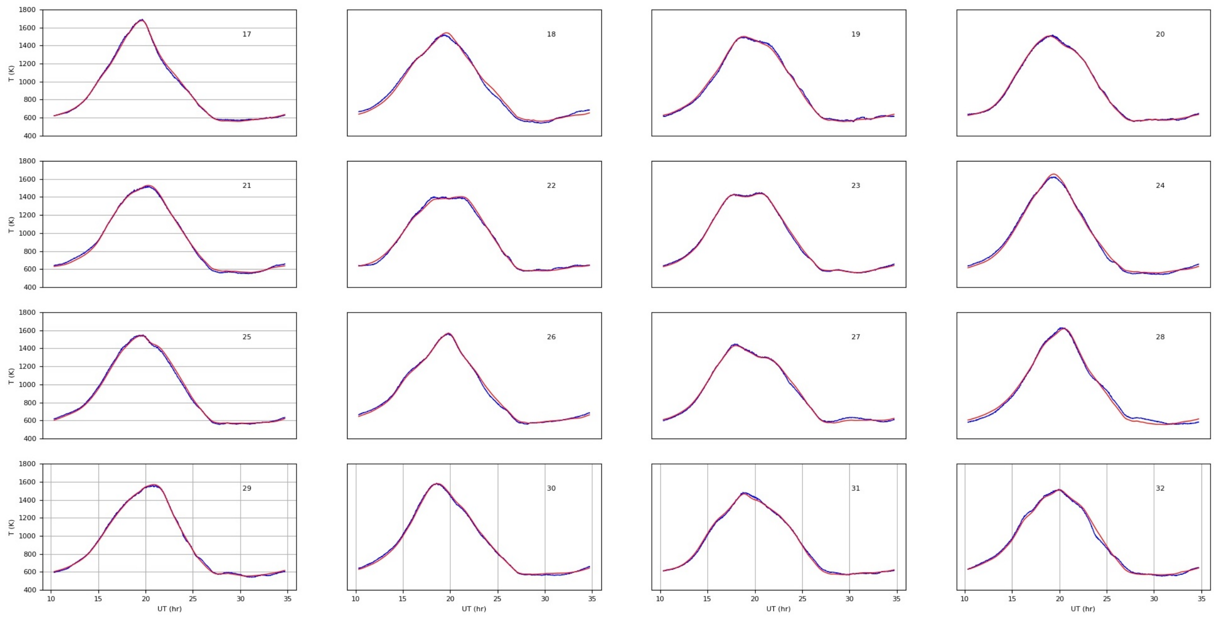

Following pages show overlays of calibrated measurements and predictions for all antennas in the AAVS2 station, in X and Y polarisations.

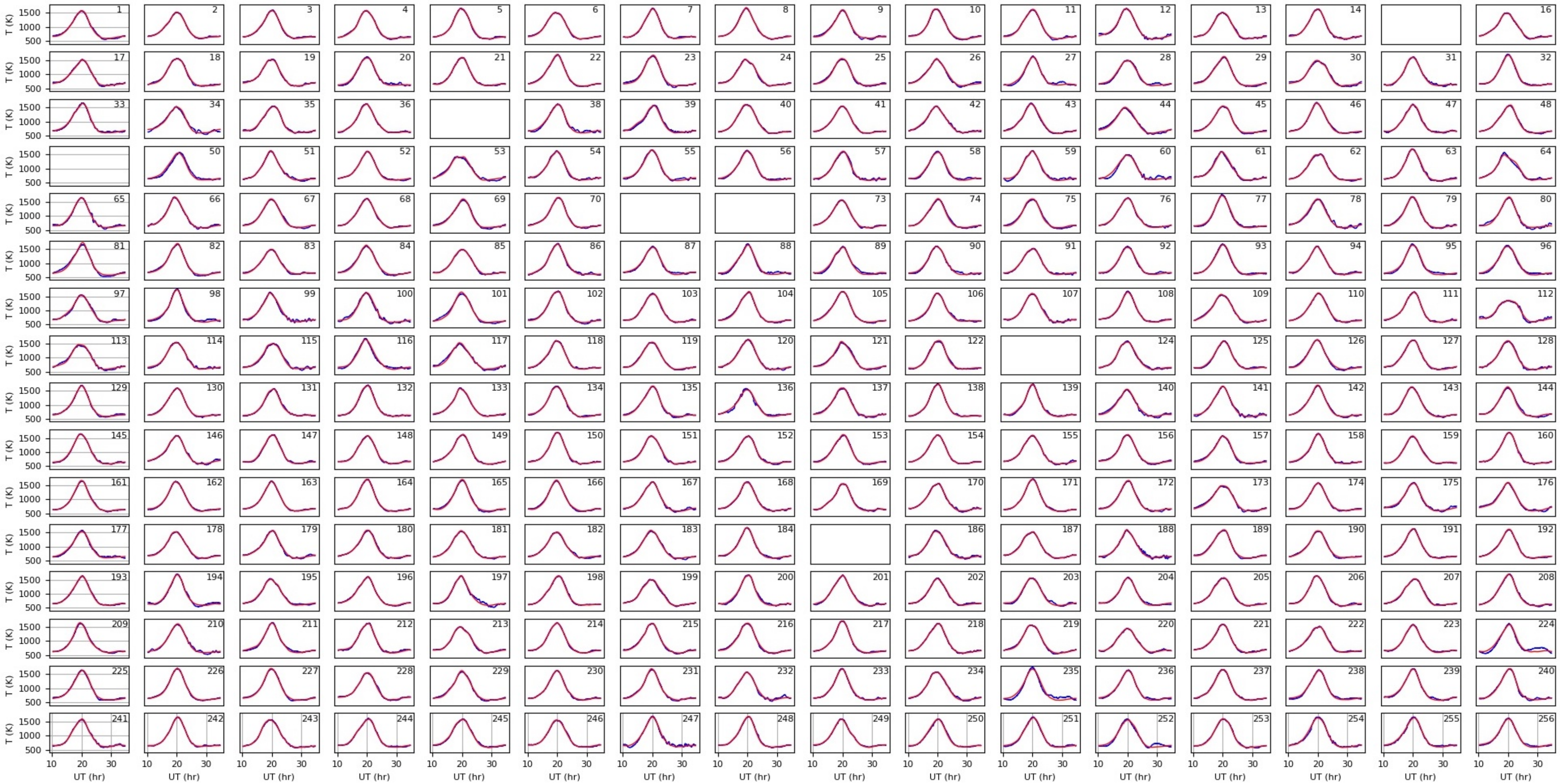
T (K)
1500
1000
500
UT (hr)
10
20
30

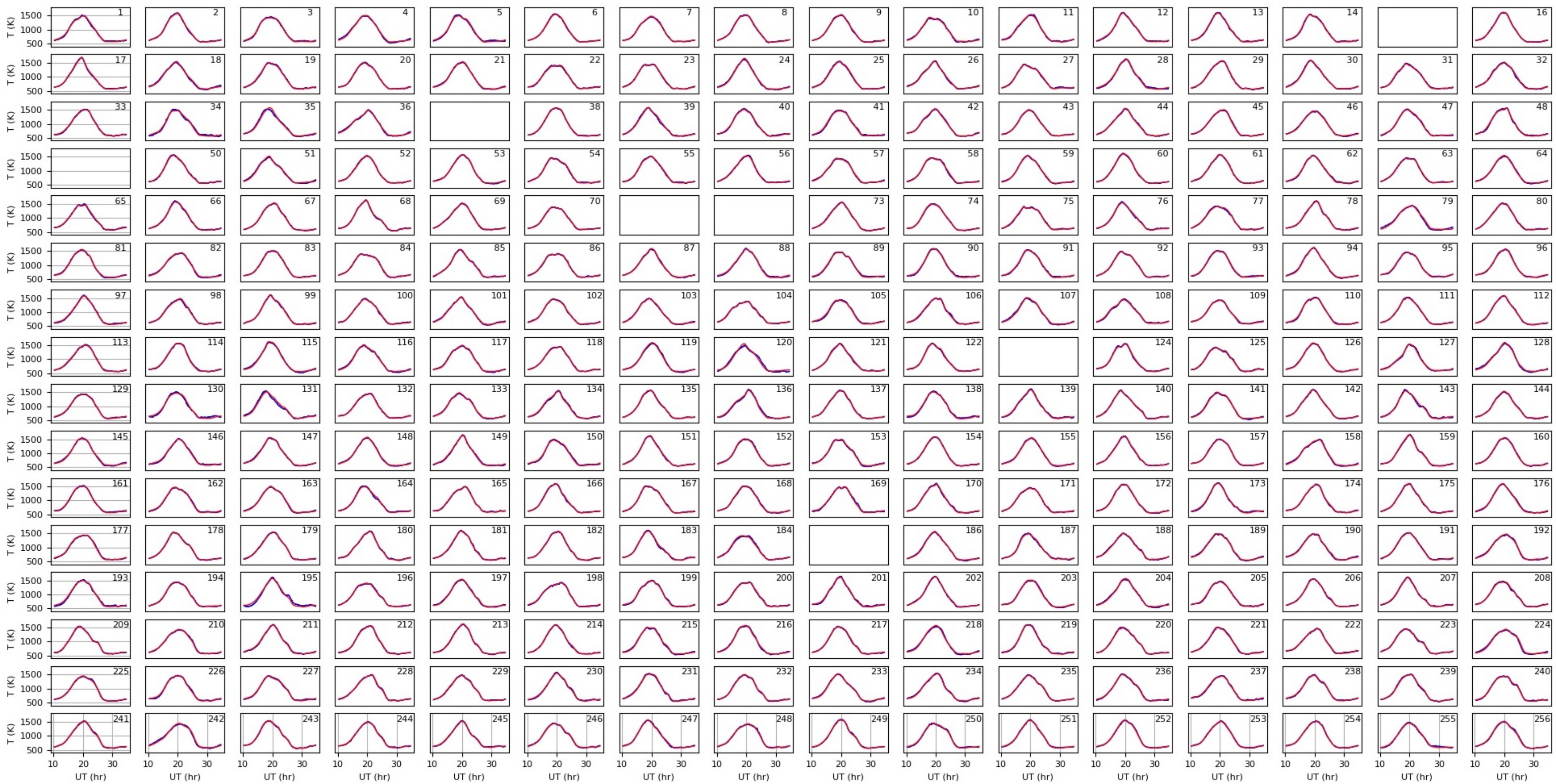
T (K)
UT (hr)

The differences between calibrated measurements and sky model predictions is most likely gain variations that is uncorrelated across the antennas of the station. Shown below are plots of this gain variation with time, for X polarisation:

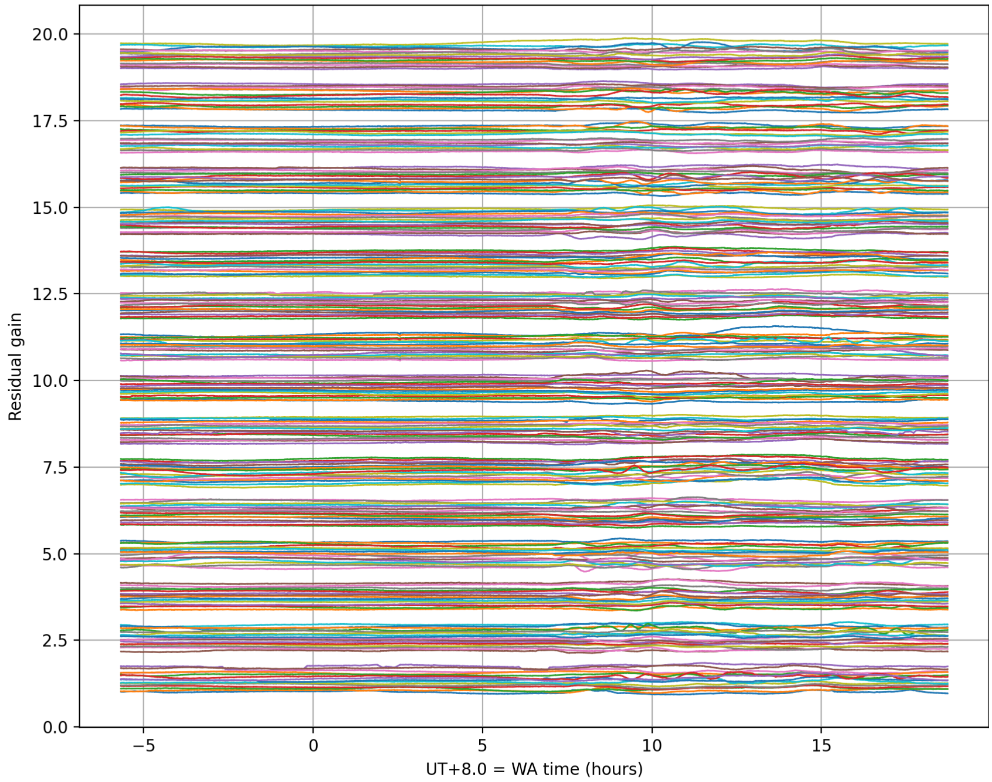

And for Y polarisation:

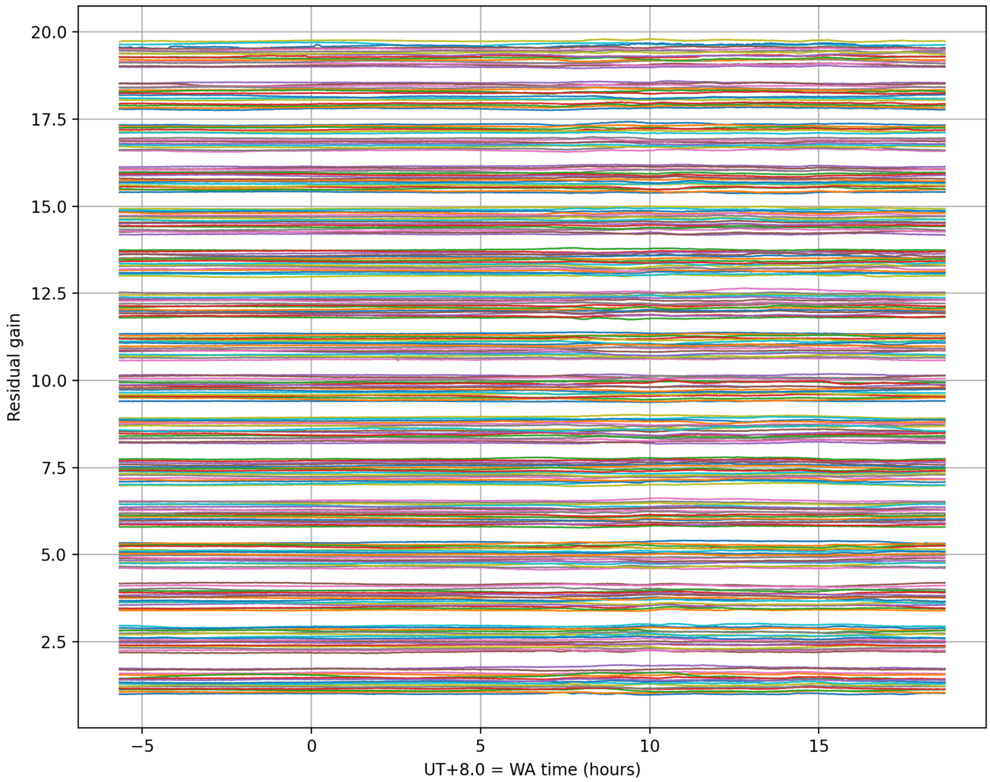

The above traces are plotted in 16 groups. Each group has gain versus time traces for 16 antennas that are all serviced by the same SMART box. Successive traces are offset vertically for clarity.

The gains of individual receiver chains are fairly smooth over the night but do show pronounced gain fluctuations during daylight hours. Presumably this is due to solar heating in some component of the receiver chain. These gain fluctuations appear uncorrelated between antennas, including between antennas that share the same SMART box. The gain fluctuations on any given antenna do not appear to be correlated between the X and Y polarisations.

The RMS of the gain fluctuations are greater in X compared to Y polarisation. The RMS of the gain fluctuations is about 0.2 dB in X and 0.1 dB in Y polarisation. It may be noted here that the peak-to-peak gain drift over the 24 hrs was also greater in X compared to Y polarisation.

I have also made plots of predictions for antenna temperature due to the Sun drifting through the antenna beams during the day. The site latitude is -26.7 degrees and during the observing session the mean position of the Sun is $RA : 01^h59^m, DEC : +12^o09^m$. Hence at meridian transit the Sun is at zenith angle of 39 degrees.

Below, on the left, is the predicted response of X polarisation beams to Sun, and on the right is that of Y polarisation beams.

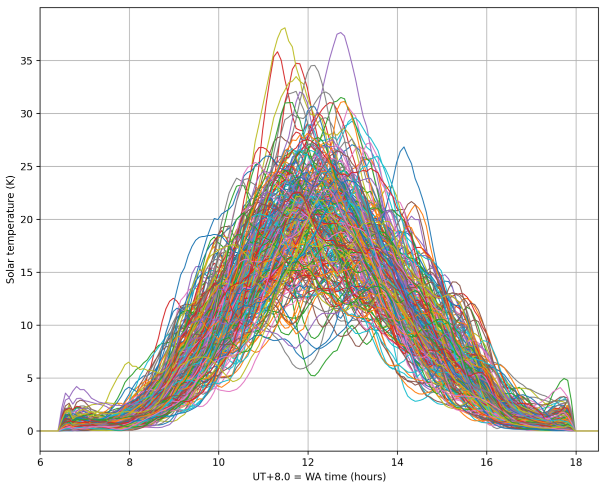

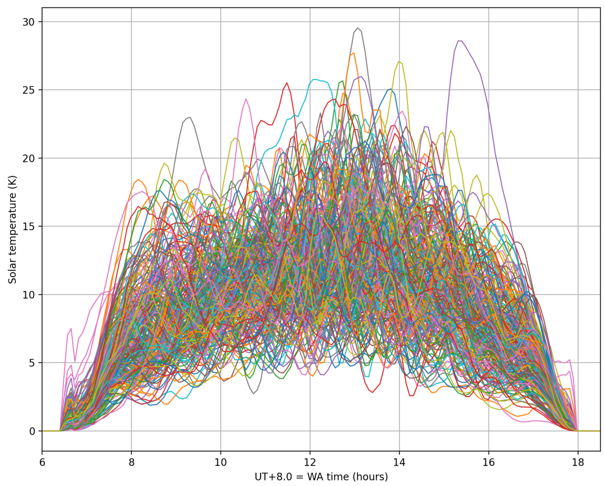

At meridian crossing, the predicted antenna temperature due to the Sun is 20 ± 5 K in X polarisation and 13 ± 4.1 K in Y polarisation, where I have quoted the 1 standard deviations of the scatter as errors. Compared to 600-1600 K from sky background, the Sun contributes at most 1-3% of the system temperature at 110 MHz, depending on the local sidereal time.

The plots above show substantial variations in antenna temperature as the Sun transits, across the antennas in the station and over time. The plots are slices of the computed embedded beam patterns in X and Y polarisation. The large scatter in antenna temperatures is due to the dissimilar and patchy nature of the EEP beams. If the station calibration is derived from intra-station correlations on the Sun, and assuming an average element pattern for the antennas of the station, then the antenna amplitude gains will suffer RMS error of 25% in X and 30% in Y polarisation.

Summary:

A. The predictions for the antenna temperatures using the global sky model and antenna embedded element patterns match reasonably well with measurement data: RMS difference is less than 3% in Y and 5% in X polarisation. Hence antenna amplitude gain calibration to within 3-5% accuracy is currently possible using global sky models and antenna total powers.

B. Current limitation to improving accuracy in AAVS2 performance verification and antenna calibration is from

   1. Slow diurnal drifts in gain of the receiver chains, with ambient temperature. The peak-to-peak gain change over 24 hr appears to be about 3 dB in X and 1.75 dB in Y polarisation.

   2. More rapid gain fluctuations during daylight hours with timescale of ~ 1 hr. This is uncorrelated between the antennas, including between those that are serviced by the same SMART boxes, and between X and Y polarisations of the same antenna. The RMS gain fluctuations is about 0.2 dB in X and 0.1 dB in Y polarisation.

It would be useful to pin down the origin for both the diurnal drift and the more rapid gain fluctuations.

The slower drift may be calibrated out with temperature monitoring and characterisation. Moreover, this slow drift of gain is common mode and hence will not change the station beam or intra-station correlations, except for a common scaling factor for the entire station.

It is, however, desirable that we fix the cause for rapid gain fluctuations, which are uncorrelated across antennas. The rapid gain fluctuations will limit accuracy of verification of field node performance, and calibration of the station beam. The rapid gain fluctuations would result in a time-varying station beam even for a drift scan observation.

C. Analysis of total powers from antennas and comparison with predictions based on global sky model and embedded patterns might be part of the verification process as SKA Low stations are built out. Such analysis verifies the computed EEP patterns and also antenna performance. The validation accuracy is today limited to 3-5% because of gain instability of the receiver chains. As the electronics gain stability is improved, the verification accuracy will correspondingly improve.

Minor issues:

1. A uniform antenna numbering scheme needs to be adopted so that the same scheme is used in labelling EM simulation and in data acquisition codes. At the moment the EEP patterns have antenna numbering different from the antenna numbers assigned by the data acquisition.

2. One antenna - numbered 211 in data files - appears to me to have a wrong location in the data files generated by the acquisition system. It corresponds to antenna number 42 in EM simulations.